

## Transport in asymmetric multiple-barrier magnetic nanostructures

Yong Guo, Binglin Gu, and Wenhui Duan

CCAST (World Laboratory), P.O. Box 8730, Beijing 100080, People's Republic of China  
and Department of Physics, Tsinghua University, Beijing 100084, People's Republic of China

Yu Zhang

Department of Physics, Tsinghua University, Beijing 100084, People's Republic of China

(Received 15 July 1996; revised manuscript received 10 October 1996)

Transport of electrons in asymmetric multiple-barrier magnetic structures is inspected in detail with transfer-matrix technique. It is found that, compared with transport in symmetric double-barrier magnetic structures, both the transmission and the conductance are drastically reduced for electrons tunneling through asymmetric double-barrier magnetic cases, and the asymmetric magnetic structure possesses stronger wave-vector filtering properties. For electrons tunneling through the nanostructure consisting of more magnetic barriers, the transmission and the conductance exhibit more complicated and sharper peaks. [S0163-1829(97)09715-4]

Electron motion in the magnetic-barrier structure has caused vast amounts of research interest. Experimentally inhomogeneous magnetic fields on the nanometer scale can be realized with the creation of magnetic dots,<sup>1</sup> the patterning of ferromagnetic materials,<sup>2</sup> and the deposition of superconducting films on heterostructures.<sup>3</sup> Theoretically, the creation of superlattices by an inhomogeneous magnetic field, transport properties of a weakly, and periodically modulated two-dimensional electron gas<sup>4</sup> (2DEG) with its elementary excitation<sup>5</sup> have been investigated. Electron motion in a stripe of a 2DEG subject to a constant magnetic field<sup>6</sup> and one in which the magnetic field increased linearly in one direction<sup>7</sup> have also been studied. Later electron tunneling through square magnetic barriers and realistic ones was studied by Matulis, Peeters, and Vasilopoulos<sup>8</sup> and You, Zhang, and Ghosh,<sup>9</sup> respectively. It is shown that the electron tunneling is an inherently two-dimensional (2D) process, and the magnetic barriers possess wave-vector filtering properties. Very recently almost at the same period, Carmona *et al.*<sup>10</sup> and Ye *et al.*<sup>11</sup> independently observed the predicted oscillatory magnetoresistance due to a commensurability effect between the classical cyclotron diameter and the period of magnetic modulation.

It is well known that for electrons tunneling through an asymmetric multiple-barrier electric structure, its features are greatly different from those for electrons tunneling through a symmetric case.<sup>12</sup> An electron's behavior in the magnetic barrier is also drastically different from that in the electric barrier case. It can be expected that there are many effects on the transport of electrons in the asymmetric magnetic barrier. Therefore, in this paper we investigate the transport of electrons in the asymmetric multiple-barrier magnetic structure. Similarities and differences between electronic transport in symmetric and asymmetric magnetic barriers are presented.

Now we consider electrons tunneling through an asymmetric double-barrier (DB) magnetic nanostructures as shown in Fig. 1(a) and a more complicated magnetic structure as shown in Fig. 1(b). In Fig. 1(a) the height and width of the left magnetic barrier and the right magnetic barrier are  $B_1$ ,  $d_1$ , and  $B_2$ ,  $d_2$ , respectively. The width of the zero field

region is  $l$ . In Fig. 1(b)  $B_1$ ,  $B_2$ , and  $B_3$  are the heights of the left magnetic barrier, the middle magnetic barrier, and the right magnetic barrier, respectively.  $d_1$ ,  $d_2$ , and  $d_3$  are their widths.  $l_1$  and  $l_2$  are the widths of two zero field regions.

First we deal with electrons tunneling through the asymmetric DB magnetic structure. The Schrödinger equation for a 2DEG in the  $(x, y)$  plane with a magnetic field  $B$  along the  $z$  direction in each region is

$$\frac{1}{2m^*} [\mathbf{P} + e\mathbf{A}_i]^2 \psi(x, y) = E \psi(x, y) \quad (i = 1, 2, \dots, 7) \quad (1)$$

where  $m^*$  is the effective mass of the electron, and the vector potential  $\mathbf{A}_i$  will be taken in the Landau gauge  $\mathbf{A}_i = (0, A_i(x), 0)$  which results in  $B_z = dA_i(x)/dx$ . For convenience we express all quantities in dimensionless units by using the cyclotron frequency  $\omega_c = eB_0/m^*$  and the magnetic length  $l_B = \sqrt{\hbar/eB_0}$  ( $B_0 = 0.1$  T). For GaAs  $m^*$  can be taken as  $0.067 m_e$  ( $m_e$  is the free-electron mass). The coordinate  $r$  is in units of  $l_B$ ,  $A_i$  in units of  $B_0 l_B$ , the energy  $E$  in units of  $\hbar\omega_c$ . The wave function can be assumed as  $\psi(x, y) = e^{iqy} \psi(x)$ , where  $q$  is the wave vector of the electron in the  $y$  direction. So we can obtain the following 1D Schrödinger equation

$$\left\{ \frac{d^2}{dx^2} - [A_i(x) + q]^2 + 2E \right\} \psi(x) = 0 \quad (2)$$

The function  $V(x) = [A_i(x) + q]^2/2$  can be interpreted as a  $q$ -dependent electric potential. In regions 1, 4, and 7, the

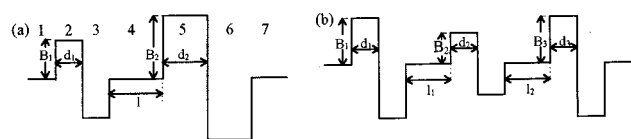


FIG. 1. (a) An asymmetric double-barrier (DB) magnetic structure. (b) A more complex magnetic-barrier structure.

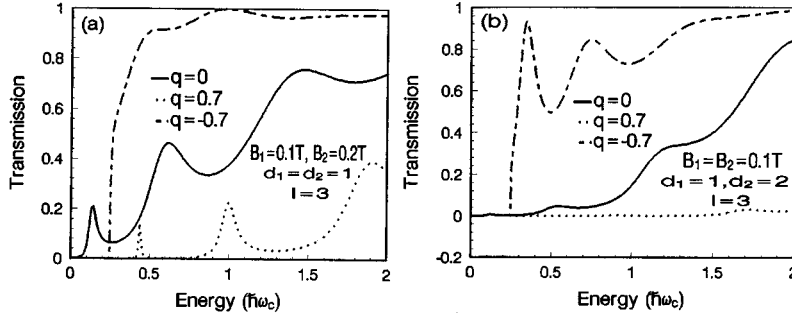


FIG. 2. The transmission coefficient through (a) a magnetic-barrier-height-induced asymmetric DB magnetic structure and (b) a magnetic-barrier-width-induced asymmetric DB magnetic structure.

wave functions are free-electron wave functions, which can be written as  $\psi_1(x) = e^{ik_1x} + re^{-ik_1x}$ ,  $\psi_4(x) = C_4 e^{ik_4x} + D_4 e^{-ik_4x}$ , and  $\Psi_7(x) = \tau e^{ik_7x}$ , respectively, where  $k_i = \sqrt{2E - [A_i(x) + q]^2}$  ( $i=1,4,7$ ).

In magnetic barrier regions 2, 3, 5, and 6, the wave function  $\psi_i(x)$  can be written as a linear combination of Hermitian functions<sup>13</sup>  $U_i^1$  and  $U_i^2$ ,

$$\Psi_i(x) = \exp\left(-\frac{\xi_i^2}{2}\right) [C_i U_i^1(\xi_i) + D_i U_i^2(\xi_i)], \quad i=2,3,5,6, \quad (3)$$

where  $C_i$ ,  $D_i$  are arbitrary constants,  $\xi_1 = \sqrt{m^* \omega_i / \hbar} (x - x_i^0)$ ,  $\omega_i = eB_z/m^*$  and

$$x_i^0 = \begin{cases} \hbar q / eB_1, & i=2 \\ 2d_1 - \hbar q / eB_1, & i=3 \\ 2d_1 + l + \hbar q / eB_2, & i=5 \\ 2d_1 + l + 2d_2 - \hbar q / eB_2, & i=6. \end{cases} \quad (4)$$

Using the transfer-matrix method, the transmission of electrons tunneling through the DB magnetic nanostructure is given by

$$T(E, q) = \frac{k_\tau}{k_1} |\tau|^2. \quad (5)$$

In the ballistic region, the conductance can be derived as the electron flows averaged over half the Fermi surface<sup>8,14</sup>

$$G = G_0 \int_{-\pi/2}^{\pi/2} T(E_F, \sqrt{2E_F} \sin \phi) \cos \phi \, d\phi, \quad (6)$$

where  $\phi$  is the angle of incidence relative to the  $x$  direction;  $E_F$  is the Fermi energy;  $G_0 = e^2 m v_F l / \hbar^2$  with  $l$  the length of the structure in the  $y$  direction and  $v_F$  the Fermi velocity.

Extension of Eqs. (5) and (6) to a more magnetic-barrier structure as depicted in Fig. 1(b) is straightforward by means of the method used above.

Figures 2(a) and 2(b) show the transmission coefficient for electrons tunneling through one magnetic-barrier-height-induced asymmetric DB structure and one barrier-width-induced asymmetric DB structure, respectively. Comparing the transmission of electrons in the symmetric DB structure [see Fig. 4(a) in Ref. 8], we can clearly see that the transmission of electrons in asymmetric magnetic structures is drastically reduced, especially for  $q=0.7$  case in which the potential profile of  $V(x)$  is equivalent to an asymmetric DB electric structure, whereas for  $q=-0.7$  the potential is an asymmetric double well. In the latter case, the transmission is due to a virtual state above a double well. It is also found that the higher the degree of the asymmetry of the structure is, the more drastically the transmission diminishes. From these results, we conclude that the asymmetric DB magnetic structure possesses inherently filtering properties for all the wave vector, and comparing with the symmetric structure, the asymmetric structure possesses stronger wave-vector filtering properties.

In order to reveal the asymmetric effect further, in Figs. 3(a) and 3(b) we present electron conductance through symmetric and asymmetric DB magnetic structures. In Fig. 3(a) we can see that for electrons tunneling through the symmetric structure the conductance has stronger and sharper resonances at the low Fermi energy region. But for electrons tunneling through the asymmetric structure, the conductance is drastically reduced and the peaks fall off rapidly with increasing the height or the width of the right magnetic barrier, and the higher the degree of the asymmetry of the structure is, the smaller the conductance will become. It can be understood that increasing the height  $B_2$  or the width  $d_2$  of the right magnetic barrier can reduce the transmission coefficient  $T(E, q)$  by altering the ‘‘trajectory’’ of the tunneling electron

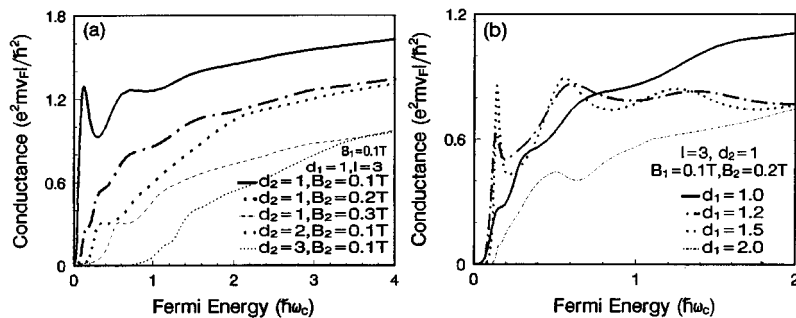


FIG. 3. (a) The conductance through the symmetric DB magnetic structure, magnetic-barrier-height-induced asymmetric DB magnetic structures, and magnetic-barrier-width-induced asymmetric DB magnetic structures. (b) The conductance through asymmetric DB magnetic structures with different widths of the left magnetic barrier and constant-width of the right barrier.

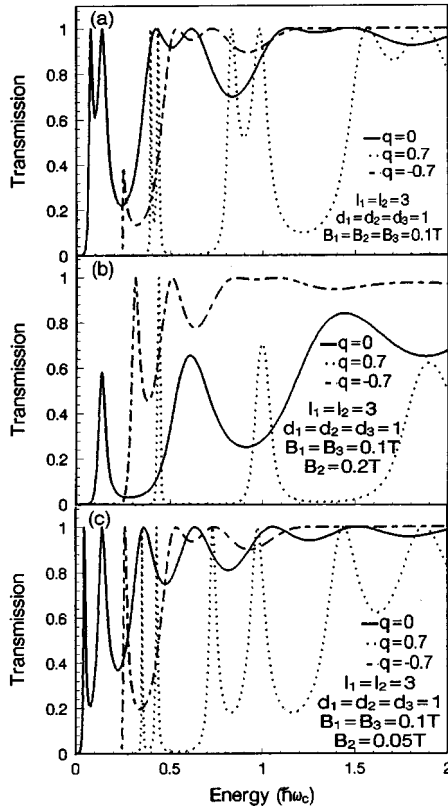


FIG. 4. (a)–(c) The transmission coefficient through one symmetric and two asymmetric more complex magnetic structures for different values of the  $y$  component of the electron wave vector  $q$ .

and increasing the effective barrier. The results of Fig. 3(b) shows the conductance through asymmetric magnetic barriers with different widths of the left barrier and constant width of the right barrier. It is found that at low Fermi energy region, the conductance first increases and the peaks become sharper, then the conductance reduces and the peaks fall off rapidly as the width of the left barriers increases. When the two barriers are of the same strength, the conductance will reach maximum and the peaks will become sharpest at low Fermi energy region. All of these phenomena can also be interpreted from the point of the symmetry of the structural effective potential.

We next calculated in Figs. 4(a)–(c) the transmission for more complicated magnetic structures depicted in Fig. 1(b). In all of our plots, solid, dotted, and dash-dotted curves represent the transmission for  $q=0$ ,  $q=0.7$ , and for  $q=-0.7$ , respectively. We can see a diminishing in the transmission peaks as the inner magnetic barriers become higher than the outer ones for  $q=0$  [analogous to the asymmetric DB magnetic case in Fig. 2(a)] and  $q=0.7$ , whereas for  $q=-0.7$ , the transmission peaks do not diminish [greatly different from the DB case in Fig. 2(a)]. In Fig. 4(b) we can also see that for  $q=0.7$  the first peak almost does not diminish, but the second and third peaks diminish drastically and the third peak falls off more rapidly than the second one. These features of the transmission for  $q=0.7$  are not only greatly different from those of the transmission for the  $q=0$  case in the same configuration, but also greatly different from those of trans-

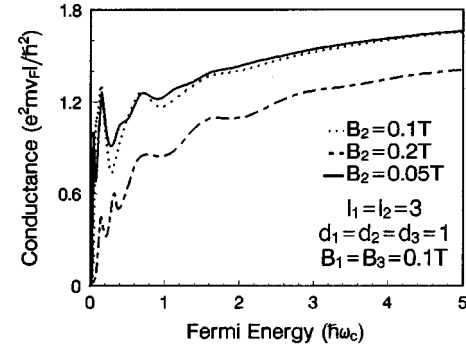


FIG. 5. The conductance through more complex symmetric and asymmetric magnetic structures. The dotted, dash-dotted, and solid curves are the calculated results for the structures which are chosen to be the same as in Figs. 4(a)–4(c).

mission for the same  $q$  value in a different configuration (i.e., the DB structure). As the inner magnetic barriers become lower than the outer barriers, what is remarkably different in this case from the previous one, where the inner barriers are higher than the outer ones, is that more and sharper resonant peaks are seen in Fig. 4(c) and the transmission peaks for all  $q$  values do not diminish.

Figure 5 shows the conductance through more complex magnetic barriers in which the structural configuration and parameters for dotted, dash-dotted, and solid curves are exactly the same as in Figs. 4(a)–(c), respectively. Despite the averaging of  $T(E, q)$  over half the Fermi surface, we have again strong resonant structure. We can see that the conductance has sharper resonant peaks at low Fermi energy region. As asymmetry is introduced by changing the height of the inner magnetic barriers lower than the outer barriers, two sharper resonances of the conductance are observed and the first peak shifts to the left. The conductance is drastically reduced and the peaks diminish for the case with the inner barriers higher than the outer barriers, whereas for the case with the inner barriers lower than the outer barriers, the conductance is enhanced in a rather wider Fermi energy range.

In summary, there exist extremely outstanding characteristics of the electronic transport in asymmetric multiple-barrier magnetic structures. Comparing with transport in symmetric DB magnetic barriers, both the transmission and the conductance are drastically reduced in asymmetric cases. The diminishing degrees of the transmission depend strongly on value and orientation of the wave vector  $\mathbf{q}$  in the  $y$  direction (i.e., positive or negative direction along the  $y$  axis). Therefore, the asymmetric DB structure possesses stronger wave-vector filtering properties. For more complex magnetic-barrier cases, the transmission and the conductance spectra exhibit more and sharper resonant peaks, and we see the strong dissimilarity between the case with the inner barriers higher than the outer barriers and the case with the inner barriers lower than the outer barriers.

This work was supported by the High Technology Research and Development Program of the People's Republic of China.

- <sup>1</sup>M. A. McCord and D. D. Awschalom, *Appl. Phys. Lett.* **57**, 2153 (1990).
- <sup>2</sup>M. L. Leadbeater *et al.*, *J. Appl. Phys.* **69**, 4689 (1991); K. M. Krishnan, *Appl. Phys. Lett.* **61**, 2365 (1992); W. Van Roy *et al.*, *J. Magn. Magn. Mater.* **121**, 197 (1993); R. Yagi and Y. Iye, *J. Phys. Soc. Jpn.* **62**, 1279 (1993).
- <sup>3</sup>A. K. Geim, *Pis'ma Zh. Eksp. Teor. Fiz.* **50**, 359 (1989) [*JETP Lett.* **50**, 389 (1990)]; S. J. Bending, K. von Klitzing, and K. Ploog, *Phys. Rev. Lett.* **65**, 1060 (1990).
- <sup>4</sup>P. Vasilopoulos and F. M. Peeters, *Superlatt. Microstruct.* **4**, 393 (1990); F. M. Peeters and P. Vasilopoulos, *Phys. Rev. B* **47**, 1466 (1993).
- <sup>5</sup>X.-G. Wu and S. E. Ulloa, *Phys. Rev. B* **47**, 7182 (1993).
- <sup>6</sup>F. M. Peeters and A. Matulis, *Phys. Rev. B* **48**, 15 166 (1993); M. Calvo, *ibid.* **48**, 2365 (1993).
- <sup>7</sup>J. E. Müller, *Phys. Rev. Lett.* **68**, 385 (1992).
- <sup>8</sup>A. Matulis, F. M. Peeters, and P. Vasilopoulos, *Phys. Rev. Lett.* **72**, 1518 (1994).
- <sup>9</sup>J. Q. You, Lide Zhang, and P. K. Ghosh, *Phys. Rev. B* **52**, 17 243 (1995).
- <sup>10</sup>H. A. Carmona *et al.*, *Phys. Rev. Lett.* **74**, 3009 (1995).
- <sup>11</sup>P. D. Ye *et al.*, *Phys. Rev. Lett.* **74**, 3013 (1995).
- <sup>12</sup>S. S. Allen and S. L. Richardson, *Phys. Rev. B* **50**, 11 693 (1994).
- <sup>13</sup>Yong Guo, Youcheng Li, Xiaojun Kong, and Chengwen Wei, *Phys. Rev. B* **50**, 7249 (1994).
- <sup>14</sup>M. Büttiker, *Phys. Rev. Lett.* **59**, 1761 (1986).